

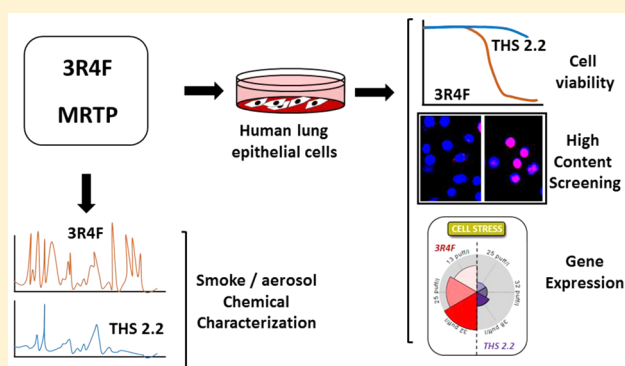
In Vitro Systems Toxicology Assessment of a Candidate Modified Risk Tobacco Product Shows Reduced Toxicity Compared to That of a Conventional Cigarette

Ignacio Gonzalez-Suarez,* Florian Martin, Diego Marescotti, Emmanuel Guedj, Stefano Acali, Stephanie Johne, Remi Dulize, Karine Baumer, Dariusz Peric, Didier Goedertier, Stefan Frentzel, Nikolai V. Ivanov, Carole Mathis, Julia Hoeng, and Manuel C. Peitsch

Philip Morris International R&D, Philip Morris Products S.A., Quai Jeanrenaud 5, 2000 Neuchâtel, Switzerland

Supporting Information

ABSTRACT: Cigarette smoke increases the risk for respiratory and other diseases. Although smoking prevalence has declined over the years, millions of adults choose to continue to smoke. Modified risk tobacco products (MRTPs) are potentially valuable tools for adult smokers that are unwilling to quit their habit. Here, we investigated the biological impact of a candidate MRTP, the tobacco-heating system (THS) 2.2, compared to that of the 3R4F reference cigarette in normal primary human bronchial epithelial cells. Chemical characterization of the THS 2.2 aerosol showed reduced levels of harmful constituents compared to those of a combustible cigarette. Multiparametric indicators of cellular toxicity were measured via real-time cellular analysis and high-content screening. The study was complemented by a whole transcriptome analysis, followed by computational approaches to identify and quantify perturbed molecular pathways. Exposure of cells to 3R4F cigarette smoke resulted in a dose-dependent response in most toxicity end points. Moreover, we found a significant level of perturbation in multiple biological pathways, particularly in those related to cellular stress. By contrast, exposure to THS 2.2 resulted in an overall lower biological impact. At 3R4F doses, no toxic effects were observed. A toxic response was observed for THS 2.2 in some functional end points, but the responses occurred at doses between 3 and 15 times higher than those of 3R4F. The level of biological network perturbation was also significantly reduced following THS 2.2 aerosol exposure compared to that of 3R4F cigarette smoke. Taken together, the data suggest that THS 2.2 aerosol is less toxic than combustible cigarette smoke and thus may have the potential to reduce the risk for smoke-related diseases.



INTRODUCTION

Cigarette smoke (CS) is harmful to nearly every organ in the body and increases the risk for cardiovascular and respiratory diseases, including lung cancer.¹ Smoking cessation is the most effective approach to minimize the risk for smoking-related diseases. For those smokers that are unwilling to quit smoking, modified risk tobacco products (MRTPs) may be a valuable tool to decrease the burden of smoke-related diseases.² Conventional cigarettes burn at temperatures around 900 °C when a puff is taken,³ resulting in partial combustion of the tobacco leaf and the generation of smoke. CS is a complex mixture with more than 8,000 identified chemicals,⁴ many of which are considered toxic or carcinogenic⁵ and suspected to be responsible for tobacco-related diseases.^{6–16} The tobacco heating system (THS) 2.2 is a candidate MRTP in which tobacco is heated rather than burned and generates a nicotine-containing aerosol by distillation. THS 2.2 is composed of an electronic holder into which a tobacco stick is inserted and heated by an electronically controlled heating blade. The stick contains a tobacco plug made of reconstituted

tobacco. The heating of the tobacco plug generates an aerosol that is primarily composed of water, glycerol, and nicotine; and contains lower levels of other harmful and potentially harmful constituents (HPHCs) that are produced when tobacco is burned.^{17–20}

Bronchial epithelial cells constitute a first-line barrier protecting the lung from inhaled harmful chemicals, such as those present in CS, thus playing a key role in the development of smoke-related diseases. We and others, have used whole genome transcriptomics to investigate the biological processes that are impacted in lung epithelial cells upon exposure to smoke from a conventional cigarette.^{21–26} Using diverse methods, the changes in gene expression were mapped in all cases to molecular pathways related to one or more of the following biological processes: xenobiotic metabolism and detoxification, oxidative stress response, inflammation, DNA damage response, apoptosis,

Received: July 31, 2015

Published: December 10, 2015

and cell cycle regulation. Taken together, the results of these studies indicate that exposure to smoke causes a very complex response in biological organisms, which results from the interaction among multiple perturbed molecular mechanisms, thus mirroring the chemical complexity of CS. As a heat-not-burn product, THS 2.2 aerosol is chemically less complex than cigarette smoke and thus may have the potential to reduce the exposure to HPHCs. However, it is still unclear whether such a reduction in HPHC levels translates into reduced toxicity.

In the present study, we used normal primary human bronchial epithelial (NHBE) cells to investigate the biological impact of THS 2.2 aerosol compared to smoke from a conventional product that is combustible, the reference cigarette 3R4F. We initially performed a chemical characterization of 3R4F smoke and THS 2.2 aerosol by measuring 58 different analytes. In addition, NHBE cells were exposed, in a time- and dose-dependent manner, to three different smoke/aerosol fractions generated from 3R4F and THS 2.2, respectively. Multiparametric indicators of cellular toxicity were measured via high content screening (HCS) analysis. The study was complemented with a microarray-based transcriptomics analysis followed by a quantitative systems biology-based approach leveraging mechanistic network models.^{27–29} This approach allowed us to identify and characterize the molecular pathways perturbed upon exposure to the different test items and to demonstrate the applicability of a systems toxicology approach to evaluate the risk associated with MRTPs.

■ EXPERIMENTAL PROCEDURES

Test Items (3R4F and THS 2.2). Reference research cigarettes 3R4F were purchased from the University of Kentucky (Lexington, KY, USA; <http://www.ca.uky.edu/refcig/>), and THS 2.2 test articles were provided by Philip Morris Products S.A. (Neuchâtel, Switzerland). The Health Canada smoking regimen (puff volume of 55 mL; puff duration of 2 s; puff frequency of 2 min⁻¹; and 100% blocking of filter ventilation holes) was used in all experiments. THS 2.2 items were puffed with a predefined puff count of 12 puffs per stick, whereas the 3R4F reference cigarettes were smoked to a butt length of 35 mm resulting with a puff count between 10 and 11 puffs per cigarette.

Chemical Characterization of Mainstream 3R4F Smoke and THS 2.2 Aerosol. Not all smoke/aerosol constituents could be measured simultaneously in all of the samples. Separate analyses were performed for the different groups described below. All constituents within each group were measured on the same smoke/aerosol samples. Descriptive statistics were performed separately for each test item (THS 2.2 and 3R4F), including the arithmetic mean and the standard deviation. A total of four determinations on four independent mainstream smoke/aerosol generations (on four different days) were performed.

Determination of Basic Analytes (Nicotine, CO, Water, Glycerol, and TPM). Analysis was performed according to ISO 4387,³⁰ 8454,³¹ and 10315.³² Briefly, mainstream 3R4F smoke and THS 2.2 aerosol samples were collected on a Cambridge glass fiber filter (44 mm diameter). TPM (total particulate matter) and CO (carbon monoxide) were determined without further treatment of the trapped aerosol. TPM was determined gravimetrically. CO was determined by nondispersive infrared photometry using a CO meter located inside the smoking machine. For nicotine, water, and glycerol determination, the filters were extracted with isopropanol containing the internal standards (*n*-heptadecane for nicotine determination and ethanol for water determination). Nicotine was analyzed by gas chromatography using flame ionization detection. Water was analyzed by gas chromatography using thermal conductivity detection. Glycerol was analyzed by gas chromatography using flame ionization detection.

Determination of Volatile and Semivolatile Constituents. Mainstream 3R4F smoke and THS 2.2 aerosol samples were collected on a Cambridge glass fiber filter connected in series with 2 cooled

microimpingers each containing 10 mL of methanol. The content of the 2 microimpingers was pooled and merged with the pad after aerosol generation. The extracts were analyzed by gas chromatography using mass spectrometry in electron impact ionization mode. The same aerosol extracts were analyzed two times, first for volatiles (1,3-butadiene, isoprene, benzene, acrylonitrile, and toluene) and second for the semivolatile determination (pyridine, styrene, and quinoline).

Determination of Aromatic Amines. Mainstream 3R4F smoke and THS 2.2 aerosol samples were collected on a Cambridge glass fiber filter and extracted with an acidic aqueous solution, which was then filtered, alkalized, and further cleaned and trace-enriched using an automatic solid-phase extraction. The eluent was derivatized with heptafluorobutyric anhydride and the levels of five aromatic amines (1-aminonaphthalene, 2-aminonaphthalene, 3-aminobiphenyl, 4-aminobiphenyl, and *o*-toluidine) analyzed by gas chromatography mass spectrometry in negative chemical ionization mode.

Determination of Nitrogen Oxides (NO and NO_x). Mainstream 3R4F smoke and THS 2.2 aerosol samples were collected in a gas collection bag. The levels of NO and NO_x were measured directly after aerosol generation using a NO meter calibrated with a certified reference NO gas (80 ppm).

Determination of Hydrogen Cyanide. Mainstream 3R4F smoke and THS 2.2 aerosol samples were collected in 2 microimpingers each containing 10 mL of 1 M sodium hydroxide solution connected in series. The content of the impingers was pooled after aerosol collection. The extracts were derivatized with 2,3-naphthalene-dicarboxaldehyde and taurine. The internal standard was derivatized *in situ* with the standards and samples. An aliquot was analyzed using liquid chromatography with tandem mass spectrometry with electron spray ionization.

Determination of Ammonia. Mainstream 3R4F smoke and THS 2.2 aerosol samples were collected on a Cambridge glass fiber filter connected in series with two microimpingers each containing 10 mL of hydrochloric acid. The content of the two microimpingers was pooled and merged with the pad. The extracts were derivatized with dansyl chloride and analyzed by liquid chromatography using tandem mass spectrometry with an atmospheric pressure chemical ionization.

Determination of Benzidine. Mainstream 3R4F smoke and THS 2.2 aerosol samples were collected on a Cambridge glass fiber filter and extracted with an acidic aqueous solution, cleaned by solid phase extraction, alkalized, and cleaned again. The eluent was derivatized with heptafluorobutyric anhydride and analyzed by gas chromatography mass spectrometry.

Determination of Epoxides and Vinyl Chloride. Mainstream 3R4F smoke and THS 2.2 aerosol samples were collected on a Cambridge glass fiber filter connected in series to one (THS 2.2) or two (3R4F) cooled microimpingers each containing 10 mL of toluene. The pad was discarded. Ethylene oxide, propylene oxide, and vinyl chloride were analyzed by gas chromatography mass spectrometry.

Determination of *N*-Nitrosamines. Mainstream 3R4F smoke and THS 2.2 aerosol samples were collected on a Cambridge glass fiber filter and extracted with ammonium acetate (100 mmol/L) containing the internal standards. After filtration, an aliquot of the aerosol extract the levels of 4-(methylnitrosamino)-1-(3-pyridyl)-1-butanone (NNK), *N'*-nitrosanornicotine (NNN), *N'*-nitrosoanatabine (NAT), and *N'*-nitrosoanabasine (NAB) were measured by liquid chromatography using tandem mass spectrometry with electron spray ionization.

Determination of Phenols and Acid Derivatives. Mainstream 3R4F smoke and THS 2.2 aerosol samples were collected on a Cambridge glass fiber filter pad connected in series with 1 cooled microimpinger containing the internal standard solution in 10 mL of butanone. For the analysis of phenols (phenol, catechol, *o*-cresol, *m*-cresol, *p*-cresol, hydroquinone, and resorcinol), the extracts were derivatized with *N,O*-bis(trimethylsilyl)-trifluoroacetamide. Acrylamide and acetamide were directly analyzed in the extract. All constituents were analyzed by gas chromatography–mass spectrometry using electron spray ionization.

Determination of Polycyclic Aromatic Hydrocarbons. Mainstream 3R4F smoke and THS 2.2 aerosol samples were collected on a Cambridge glass fiber filter and extracted with hexane. The eluate was cleaned up by two solid-phase extraction cartridges (NH₂ and C-18

phase), and the levels of benzo[*a*]pyrene, benz[*a*]anthracene, dibenz[*a,h*]anthracene, and pyrene were analyzed by gas chromatography–mass spectrometry.

Determination of Nitro Benzene. Mainstream 3R4F smoke and THS 2.2 aerosol samples were collected on a Cambridge glass fiber filter connected in series with a cartridge. The aerosol collected on the cartridge was spiked with internal standard, washed with pentane, and then eluted with a pentane/ether/isooctane (85/15/1) solution. The eluate was subsequently blown down by flushing with nitrogen and then diluted with pentane. The solution was cleaned up by an amino propyl solid-phase extraction cartridge and analyzed by gas chromatography–mass spectrometry.

Determination of Metals (Excluding Mercury). Mainstream 3R4F smoke and THS 2.2 aerosol samples were collected on an electrostatic trap and extracted with nitric acid followed by microwave digestion treatment after the addition of hydrogen peroxide. The levels of arsenic, cadmium, chromium, lead, nickel, and selenium were analyzed directly in the digested aerosol solution by inductively coupled plasma mass spectrometry. All used equipment for the analysis is located in an ISO 7 classified clean room.³³

Determination of Mercury. Mainstream 3R4F smoke and THS 2.2 aerosol samples were collected on a Cambridge glass fiber filter connected in series with 2 impingers containing nitric hydrochloric acid–internal standard–gold solution. In addition, a third impinger containing sodium bicarbonate solution was connected to protect the pump of the smoking machine. The third was not used for trapping purposes. The pad was discarded after aerosol generation. The trapped aerosols were diluted and analyzed by inductively coupled plasma mass spectrometry. All used equipment for the analysis is located in an ISO 7 classified clean room.³³

Determination of Carbonyls. Mainstream THS2.2 was collected using three microimpingers, each containing 10 mL of 2,4-dinitrophenylhydrazine (DNPH) derivatization solution connected in series to the smoking machine. The mainstream smoke from the 3R4F was collected using two impingers connected in series to the smoking machine. Samples were allowed to stabilize for 30 min and then quenched by adding pyridine. Derivatized solutions were transferred to acetonitrile containing an internal standard mixture (butanone-*d*₅ and acetone-*d*₆). The concentration of formaldehyde, acetaldehyde, acetone, acrolein, propionaldehyde, crotonaldehyde, 2-butanone, and butyraldehyde was measured by liquid chromatography–electrospray ionization tandem mass spectrometry.

Cell Culture. NHBE cells were purchased from Lonza (Catalog no. CC-2540, Lonza, Cologne, Germany). The donor was a 60-year-old Caucasian male with no history of smoking (ref: CC2540, lot number 0000140733). Replicating bronchial epithelial cells have a normal karyotype.³⁴ For all experiments described here, we used cells between passages five and eight. The cells were maintained in a humidified incubator at 37 °C and 5% CO₂ and cultured in bronchial epithelial cell medium (Bullet Kit CC 3170, Lonza) as previously described.³⁵ Briefly, cells were seeded in uncoated T75 flasks with 20 mL of medium at a density of 50,000 cells/mL grown until 80% confluence changing the medium every 2 days.

Preparation of Smoke/Aerosol Fractions for Cell Exposure. In order to expose NHBE cells to 3R4F and THS 2.2, three different fractions were prepared from mainstream smoke/aerosol: an aqueous extract (AE), TPM, and gas-vapor phase (GVP).

AE was prepared by bubbling mainstream 3R4F smoke or THS 2.2 aerosol through ice-cold phosphate buffered saline (PBS) in a wash bottle, thus trapping the water-soluble fraction. For 3R4F, mainstream smoke from a total of six cigarettes was trapped in 36 mL of PBS. For the THS 2.2, mainstream smoke from a total of 10 cigarettes was trapped in 40 mL of PBS.

TPM was prepared by collecting mainstream 3R4F smoke and THS 2.2 aerosol on Cambridge glass fiber filters (44 mm diameter). For 3R4F, mainstream smoke from a total of six cigarettes, divided in two batches of three items, was trapped on two separate glass fiber filters followed by extraction with 5 mL of ethanol in a plastic vessel. For the THS 2.2, mainstream aerosol from a total of 10 sticks, divided into 2 batches of 5 sticks, was trapped on 2 separate glass fiber filters followed

by extraction with 5 mL of ethanol in a plastic vessel. For both items, the first filter was extracted with 5 mL of ethanol. The second filter was extracted with the first crude extract.

GVP is defined as the substance that passes through the glass fiber filter during TPM collection. GVP was collected by bubbling mainstream 3R4F smoke or THS 2.2 aerosol through ice-cold PBS in a wash bottle. For 3R4F, mainstream smoke from a total of 6 cigarettes, divided into 2 batches of three items, was trapped in 36 mL of PBS. For the THS 2.2, mainstream smoke from a total of 10 sticks, divided into 2 batches of 5 items, was trapped in 40 mL of PBS.

The AE and GVP stock solutions generated from 3R4F smoke contained the equivalent of 167 cigarettes per liter (approximately 1,750 puffs/L). The AE and GVP stock solutions generated from THS 2.2 aerosol contained the equivalent of 250 sticks per liter (approximately 3,000 puffs/L). The TPM stock solution generated from 3R4F smoke contained the equivalent of 1,200 cigarettes per liter (approximately 12,575 puffs/L). The TPM stock solution generated from 3R4F smoke contained the equivalent of 2,000 cigarettes per liter (approximately 24,000 puffs/L). All stock solutions were prepared fresh prior to each experiment, and they were diluted in cell culture medium and used for cellular exposure within 30 min of generation.

Determination of Carbonyls in GVP and AE Fractions. In order to QC the generation of smoke/aerosol fractions and to monitor batch-to-batch variability, carbonyls were measured in AE and GVP stock solutions. Carbonyls were not determined in TPM as these compounds are typically not present in the particulate. A 400 μ L aliquot of the AE and GVP stock solutions was collected immediately after generation and derivatized with DNPH solution. Samples were allowed to stabilize for 30 min and then quenched with pyridine. Derivatized solutions were transferred to acetonitrile containing an internal standard mixture (butanone-*d*₅ and acetone-*d*₆). The concentration of formaldehyde, acetaldehyde, acetone, acrolein, propionaldehyde, crotonaldehyde, 2-butanone, and butyraldehyde was measured by liquid chromatography–electrospray ionization tandem mass spectrometry. Descriptive statistics were performed separately for each test item (THS 2.2 and 3R4F), including the arithmetic mean and the SEM of a total of eight determinations on eight independent mainstream smoke/aerosol generations (on eight different days).

Cell Viability. Cell viability was measured using a multielectrode array-based real-time cellular analysis (RTCA) system (ACEA Biosciences Inc., San Diego, CA, USA). NHBE cells were seeded into E-Plate View 96-well tissue culture plates (ACEA Biosciences) at a density of 7.2×10^3 cells per well in 100 μ L of culture medium and incubated for 24 h at 37 °C and 5% CO₂. Cells were then exposed (in triplicate) to seven different concentrations of each smoke/aerosol fraction for an additional 24 h. Appropriate positive (carbonyl cyanide *m*-chlorophenyl hydrazone) and vehicle controls (2% ethanol or PBS) were included in each experiment. Cell viability, measured as change in impedance over time, was monitored and recorded throughout the duration of the experiment. At least three independent experiments with independently generated smoke/aerosol fractions were performed.

High Content Screening. Experiments were performed as previously described.³⁵ Briefly, NHBE cells were seeded in black, clear-bottomed 96-well tissue culture plates at a density of 12,000 cells per well (3,000 cells per well for the cell cycle end point). The cells were incubated for 24 h in the culture medium and then exposed (in three replicate wells) to increasing doses of the different smoke/aerosol fractions or the vehicle control (PBS or 2% ethanol). The cells were exposed for 4 or 24 h before running the HCS assays (only the 24 h time point was used for the cell cycle analysis end point). In parallel, appropriate positive controls were used for each assay: carbonyl cyanide *m*-chlorophenyl hydrazone for mitochondrial membrane potential and mitochondrial mass (MitoTracker, Life Technologies, Carlsbad, CA, USA) apoptosis (caspase 3/7 activity CellEvent, Life Technologies), cell membrane permeability (YO-PRO-1, Life Technologies) and cytochrome C release (antibody, Abcam, Cambridge, UK); tacrine for reactive oxygen species (dihydroethidium, Sigma, St. Louis, MO, USA); nocodazole and aphidicolin for the cell cycle (5-ethynyl-2'-deoxyuridine, EDU, Sigma); ethacrynic acid for glutathione content (monochlorobimane, Sigma); mitomycin C for DNA damage

(phospho-H2AX antibody, Millipore, Billerica, MA, USA); and colchicine for MAPK signaling (p-cJun antibody, Millipore). DMSO (0.5%) was used as the vehicle control for all control treatments. Cell count, nuclear size, and DNA structure were measured in all assays using Hoechst 33342 (Life Technologies). Following staining of the NHBE cells, fluorescence was analyzed by image acquisition with a Thermo Fisher Cellomics ArrayScan VTI High Content Screening Reader (Thermo Fisher Scientific, Waltham, MA, USA) and vHCSTMview software (Thermo Fisher Scientific). Twenty fields were imaged per well using a 10× wide field objective as previously described.³⁶ Table 1

Table 1

assay	end point	biological end point	cellular compartment	output feature
cytotoxicity	1	mitochondrial mass	cytoplasm	spot average area
	2	mitochondrial membrane potential	cytoplasm	spot average intensity
	3	cytochrome C release	nucleus	average intensity
	4	cell membrane permeability	nucleus	average intensity
DNA damage	5	phospho-H2AX	nucleus	average intensity
stress kinase	6	phospho-cJun	nucleus	average intensity
ROS	7	ROS	nucleus	average intensity
GSH content	8	GSH	cytoplasm	spot average intensity
apoptosis	9	caspase 3/7	cytoplasm	spot average intensity
cell cycle	10	DNA content	nucleus	average intensity

indicates, for each end point, the cellular compartment where the end point is measured as well as the output feature used by the software for quantification. At least three independent experiments (with three independent fraction generations on different days) were performed for each test item and assay. A one-sample *t* test was used with the null hypothesis that the population mean is equal to 1.

RNA Extraction and Microarrays Hybridization. NHBE cells were seeded in black, clear-bottomed 96-well tissue culture plates at a density of 12000 cells per well. The cells were incubated for 24 h in the culture medium and then exposed (in four replicates) for 4 h to the selected doses of the different smoke/aerosol fractions or vehicle control (PBS or 2% ethanol). Cells were subsequently lysed using RLT (Qiagen AG, Hilden, Germany), which contains 1% beta mercaptoethanol, and isolation of RNA was performed with the RNeasy microkit (Qiagen AG). For each dose, four replicate wells were pooled together for RNA extraction. The concentration of the isolated RNAs was measured by a NanoDrop ND8000 Spectrophotometer (Thermo Fisher Scientific). RNA quality was verified using an Agilent 2100 Bioanalyzer (Agilent, Santa Clara, CA, USA). The minimum RNA integrity number was 6.9 (the average value in this study was 9.5). For mRNA analysis, 50 ng of total RNA was processed as described in the Nugen Ovation RNA Amplification system V2 protocol (Nugen, San Carlos, CA, USA). A Genechip Human Genome U133 Plus 2.0 Array (Affymetrix, Santa Clara, CA, USA) was used for hybridization, which simultaneously probed the expression of thousands of genes. The total number of RNA samples analyzed was 74. Three biological replicates (three independent experiments with three independent smoke/aerosol generations on different days) were collected for each test item, fraction, and concentration. The number of technical replicates per experiment was one. Within each experiment, all RNA samples were processed in the same batch. Raw CEL files were background-corrected, normalized, and summarized using frozen-Robust Microarray Analysis (fRMA).³⁷ Background correction and quantile normalization were used to generate microarray expression values from all arrays passing quality

control checks using the custom CDF environment HGU133Plus2_Hs_ENTREZG v16.0.³⁸ A log-intensities plot, normalized-unscaled standard error plot, relative log expression plot, polyA controls boxplot, RNA degradation plot, spike-in controls boxplot, and pseudo and raw images using R packages were generated for quality checks (AffyPLM; Bioconductor, Seattle, WA, USA).^{39,40} The gene expression data used in this publication have been deposited in ArrayExpress (<http://www.ebi.ac.uk/arrayexpress/>) and are accessible through accession number E-MTAB-3738.

To identify genes with differential expression following treatment, a linear model was defined: expression = $\beta_0 + \beta_1 \times (\text{dose/stick-type/fraction}) + \epsilon$; for every dose/stick type/fraction (DSF), we fitted a model to the samples in the DSF group and the corresponding control group. The coefficient β_1 is equivalent to a pairwise comparison, DSF – vehicle_(DSF). β_0 is the intercept, and ϵ is the error term. The β coefficients were estimated using the Limma R package.⁴¹ Doses were not fitted in a single model as strong heteroscedasticity between dose and exposure time was expected. A heatmap of the log2 transformed gene expression fold changes (FC) between samples exposed to each fraction and the corresponding samples exposed to the vehicle control was generated using the heatmap.2 function in the gplots R package.⁴² A gene was defined as differentially expressed only if its $|\text{FC}| > \log_2(1.2)$ and its $\text{fdr} < 0.05$. FC was set to be zero for all the nondifferentially expressed genes. Negative and positive FCs were indicated in cyan and yellow, respectively. Hierarchical clustering was performed using the hclust function in the “stats” R program.⁴³

Ingenuity Pathway Analysis. Core analyses using the QIAGEN Ingenuity Pathway Analysis (IPA) software (content version: 14718999, release date: 14 September 2015, QIAGEN, Redwood City, CA, USA) were performed using a FC cutoff of log2(1.2) and an fdr cutoff of 0.1. A comparison analysis was generated to compare the canonical pathways across all groups. Filters were set for all of the apoptosis related signaling pathways, for cell cycle regulation, for cellular growth, for proliferation and development, for cellular stress and injury, for growth factor signaling, for intracellular and second messenger signaling, for nuclear receptor signaling, for transcriptional regulation, and for xenobiotic metabolism. The comparison analysis was visualized in a heatmap displaying the negative log10-transformed *p*-value derived from the Fisher's exact test.

Network-Based Analysis. Network Perturbation Amplitude (NPA). Gene expression profiles induced by exposure to the different smoke/aerosol fractions were analyzed in the context of a collection of hierarchically structured network models describing the molecular mechanisms underlying the essential biological processes in healthy lung tissues.²⁷ Cell proliferation,⁴⁴ inflammation,⁴⁵ cellular stress,⁴⁶ and cellular fate.⁴⁷ All networks are available⁴⁸ at <http://www.causalbionet.com>. Leveraging the “cause-and-effect” network models together with NPA algorithms, the gene expression fold-changes were translated into differential values for each network node. The node differential values were in turn summarized into a quantitative measure of NPA as previously described.^{49,50} The network models and their corresponding subnetworks that were used in the study are listed in Table S1.

Biological Impact Factor (BIF). The network models represent functionally distinct biological processes characterizing the systems under consideration. The exposure impact on these biological processes was further quantified in terms of a systems-wide and pan-mechanistic metric of biological impact, the BIF.^{27,29} To objectively evaluate the overall biological impact relative to a reference within the experiment, the weighted sum of the significant network perturbations for the contrast are normalized with respect to the corresponding weighted sum for the reference.^{29,49}

RESULTS

Reduced HPHC Levels in Mainstream THS 2.2 Aerosol Compared to That in 3R4F Smoke. To determine whether heat-not-burn technology results in lower HPHC levels compared to that of conventional cigarettes, we performed a chemical characterization of 3R4F smoke and THS 2.2 aerosol (Table 2). Both test items showed similar values for TPM,

Table 2. Chemical Characterization of 3R4F Smoke and THS 2.2 Aerosol^a

	parameters	units	3R4F	THS 2.2	THS 2.2 vs 3R4F (%)
1	NFDPM	mg/stick	31.2 ± 0.6	10.3 ± 0.3	−67%
2	glycerol	mg/stick	2.42 ± 0.04	4.63 ± 0.26	−91%
3	TPM	mg/stick	49 ± 1.5	48.2 ± 0.8	−2%
4	nicotine	mg/stick	1.89 ± 0.05	1.32 ± 0.05	−30%
5	water	mg/stick	15.8 ± 0.9	36.5 ± 1	+131%
6	carbon monoxide	mg/stick	32.8 ± 0.7	0.531 ± 0.021	−98%
Aliphatic Dienes					
7	1,3-butadiene	μg/stick	63.8 ± 1.1	0.294 ± 0.013	−99.9%
8	isoprene	μg/stick	798 ± 15	2.35 ± 0.12	−99.9%
Carbonyls					
9	formaldehyde	μg/stick	56.5 ± 3.8	5.53 ± 0.22	−90%
10	acetaldehyde	μg/stick	1555 ± 38	219 ± 10	−86%
11	acetone	μg/stick	736 ± 41	40.7 ± 1.9	−94%
12	acrolein	μg/stick	154 ± 6	11.3 ± 0.7	−93%
13	propionaldehyde	μg/stick	125 ± 5	14.5 ± 0.7	−88%
14	crotonaldehyde	μg/stick	68.8 ± 4.5	4.14 ± 0.07	−94%
15	methyl-ethyl-ketone	μg/stick	187 ± 9	7.18 ± 0.37	−96%
16	butyraldehyde	μg/stick	88.4 ± 3.4	26.1 ± 0.7	−70%
Acid Derivatives					
17	acetamide	μg/stick	13.9 ± 0.2	4.02 ± 0.06	−71%
18	acrylamide	μg/stick	4.83 ± 0.08	1.73 ± 0.04	−64%
19	acrylonitrile	μg/stick	31.9 ± 0.6	0.258 ± 0.013	−99%
Epoxides					
20	ethylene oxide	μg/stick	29.4 ± 0.6	0.201 ± 0.004	−99%
21	propylene oxide	μg/stick	1.32 ± 0.04	0.148 ± 0.006	−89%
Nitro Compounds					
22	nitrobenzene	ng/stick	8.62 ± 0.35	<0.188* ± *	−98%
Aromatic Amines					
23	1-aminonaphthalene	ng/stick	20.8 ± 0.4	0.077* ± *	−99%
23	2-aminonaphthalene	ng/stick	11 ± 0.2	0.046 ± 0.002	−99%
24	3-aminobiphenyl	ng/stick	3.77 ± 0.15	<0.032* ± *	−99%
25	4-aminobiphenyl	ng/stick	3.26 ± 0.04	<0.051* ± *	−99%
26	<i>o</i> -toluidine	ng/stick	85.5 ± 0.8	1.26 ± 0.06	−99%
27	benzidine	ng/stick	<0.017* ± *	<0.014* ± *	N/A
<i>N</i> -Heterocyclic Aromatics					
28	pyridine	μg/stick	36.1 ± 0.7	7.54 ± 0.08	−79%
29	quinoline	μg/stick	0.513 ± 0.007	<0.012* ± *	−98%
Halogen Compounds					
30	vinyl chloride	ng/stick	96.7 ± 0.6	<3.54* ± *	−96%
Inorganic Compounds					
31	ammonia	μg/stick	39.3 ± 1	14.2 ± 0.3	−64%
32	nitrogen oxide	μg/stick	491 ± 12	16.8 ± 0.7	−97%
33	nitrogen oxides	μg/stick	537 ± 14	17.3 ± 0.8	−97%
34	hydrogen cyanide	μg/stick	493 ± 24	4.81 ± 0.11	−99%
Monocyclic Aromatics					
35	benzene	μg/stick	97.6 ± 1.5	0.649 ± 0.023	−99%
36	styrene	μg/stick	24.5 ± 0.4	0.608 ± 0.018	−98%
37	toluene	μg/stick	188 ± 4	2.59 ± 0.14	−99%
<i>N</i> -Nitrosamines					
38	<i>N</i> -nitrosonornicotine	ng/stick	309 ± 13	17.2 ± 0.4	−94%
39	<i>N</i> -nitrosoanatabine	ng/stick	318 ± 23	20.5 ± 0.1	−94%
40	<i>N</i> -nitrosoanabasine	ng/stick	33.7 ± 2.7	<3.15* ± *	−90%
41	4-(<i>N</i> -nitrosomethylamino)-1-(3-pyridyl)-1-butanone	ng/stick	266 ± 5	6.67 ± 0.19	−97%
Phenols					
42	phenol	μg/stick	13.6 ± 0.3	1.16 ± 0.04	−91%
43	<i>o</i> -cresol	μg/stick	4.47 ± 0.05	0.069 ± 0.003	−98%
44	<i>m</i> -cresol	μg/stick	3.03 ± 0.02	0.029 ± 0.001	−99%
45	<i>p</i> -cresol	μg/stick	9.17 ± 0.14	0.072 ± 0.003	−99%
46	catechol	μg/stick	91.4 ± 1.8	16.3 ± 0.5	−82%
47	resorcinol	μg/stick	1.85 ± 0.02	0.041 ± 0.001	−98%
	hydroquinone	μg/stick	83.1 ± 1.7	8.1 ± 0.15	−90%

Table 2. continued

	parameters	units	3R4F	THS 2.2	THS 2.2 vs 3R4F (%)
PAHs					
48	benzo[<i>a</i>]pyrene	ng/stick	14.2 ± 0.1	<1.00* ± *	−93%
49	pyrene	ng/stick	87.3 ± 0.8	<5.00* ± *	−94%
50	benzo(<i>a</i>)anthracene	ng/stick	28 ± 0.2	1.45 ± 0.04	−95%
51	dibenzo(<i>a,h</i>)anthracene	ng/stick	1.7 ± 0.03	<0.100* ± *	−94%
Metals/Elements					
52	arsenic	ng/stick	8.51 ± 0.11	<1.13* ± *	−87%
53	cadmium	ng/stick	161 ± 1	<0.350* ± *	−99%
54	chromium	ng/stick	<0.550* ± *	<0.550* ± *	N/A
55	lead	ng/stick	37 ± 0.2	<3.35* ± *	−91%
56	mercury	ng/stick	4.8 ± 0.04	1.17 ± 0.02	−76%
57	nickel	ng/stick	<0.550* ± *	<0.550* ± *	N/A
58	selenium	ng/stick	1.62 ± 0.1	<0.550* ± *	−66%

^aValues represent the average ± standard deviation of four determinations (on four different days). Values in the top right column represent the percentage of change (increase or decrease) of a particular parameter in THS 2.2 compared to that of 3R4F. * Indicates that a value was below the limit of quantification (LOQ) of the method. In those cases, the LOQ value was used to calculate the percentage of change. When a parameter had LOQ values for both test items, the percentage of change could not be calculated and is indicated as N/A. NFDPM: nicotine-free dry particulate matter (tar). PAH: polycyclic aromatic hydrocarbons.

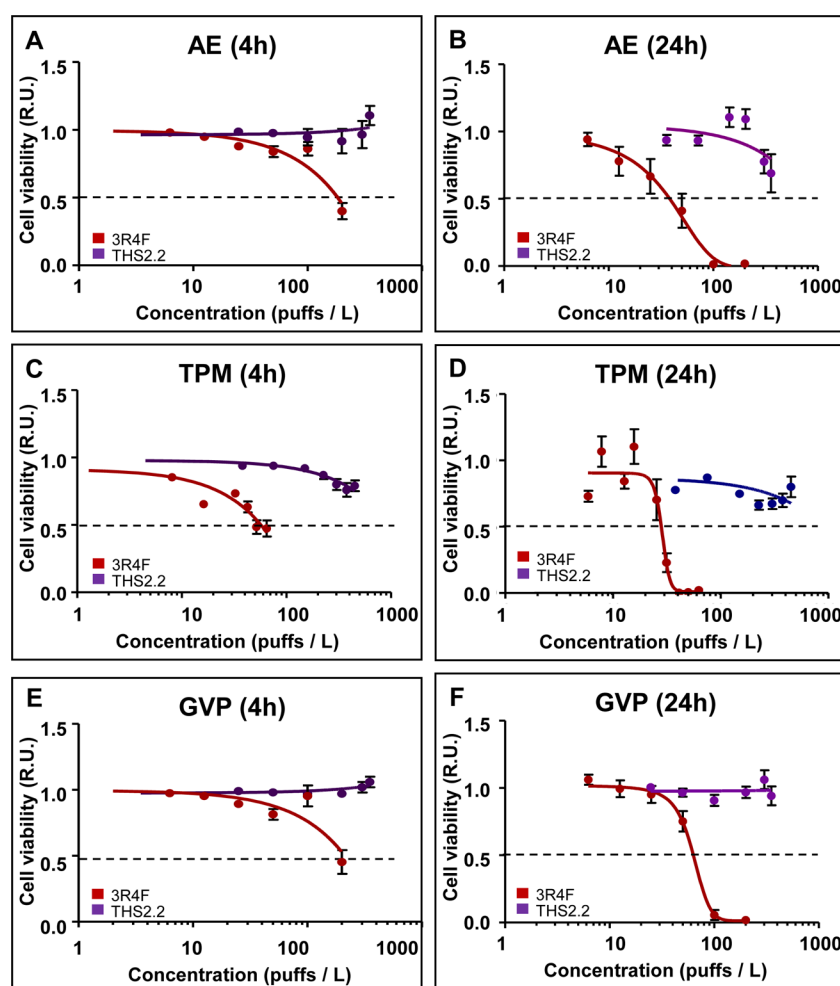


Figure 1. Cell viability in NHBE cells exposed for 4 h or 24 h to AE (A and B), TPM (C and D), or GVP (E and F) fractions from 3R4F smoke or THS 2.2 aerosol. Values are normalized to the vehicle control and represent the average ± SEM of at least three independent experiments. The dotted line indicates 50% cell viability. R.U. relative units.

although there were major differences in fraction composition. TPM is mostly composed of liquid droplets containing water, nicotine, and a nicotine-free dry particulate matter (NFDPM), also referred to as tar. In the case of 3R4F, the TPM fraction

contains 64% of NFDPM (31.2 mg/stick) and 32% water (15.8 mg/stick). In contrast, THS 2.2 TPM contains more than 75% water (36.5 mg/stick) and only 20% of NFDPM (10.3 mg/stick). Nicotine levels are approximately 30% higher in 3R4F

Table 3. Summary of HCS Results^a

end point	exposure	s/aPBS		TPM		GVP	
		3R4F	THS 2.2	3R4F	THS 2.2	3R4F	THS 2.2
cell loss	4 h						
	24 h	100	200*	33		200	
p-H2AX	4 h	200**		52		200**	
	24 h	200**		8	226	200**	
p-cJun	4 h			33**			
	24 h	100	200*	33		100	
ROS formation	4 h			N/A			
	24 h	100*		N/A	350	200**	
GSH content	4 h	50		33*		50	350
	24 h	100	200*	42		200	
cell cycle	4 h	13	140	8	150	25	200
	24 h			N/A	380*		
caspase 3/7	4 h			N/A			
	24 h			N/A	280	200*	300*
cytochrome C release	4 h						
	24 h	100	280*	42	380*	200**	
cell membrane permeability	4 h	100	350**	65		200*	
	24 h	100		8	150	100	350*
mitochondrial membrane potential	4 h			16	380*		
	24 h	100	280	62	280	200	
mitochondrial mass	4 h	50*				200*	
	24 h	200**			280	200*	

^aOnly end points for which a positive response was observed in at least one experimental condition are listed. Values indicate the minimum concentration (puffs/L) at which at least a 2-fold increase in signal above vehicle was observed (50% decrease for cell count, GSH content, and mitochondrial membrane potential). Cell cycle values represent the minimum concentration at which a 50% decrease in the percentage of cells in S-phase was observed. * indicates a weak response (1.5–2.0-fold increase in signal above vehicle or 30–50% decrease in cell count, GSH, and mitochondrial membrane potential). ** indicates that the response was not dose-dependent. Caspase 3/7 activity and ROS formation could not be measured in 3R4F TPM because of interferences in fluorescence emission (N/A).

(1.89 mg/stick) than in THS 2.2 (1.32 mg/stick). However, THS 2.2 has a higher proportion of glycerol, added to the tobacco stick as an aerosol former, than 3R4F (4.63 mg/stick Vs. 2.42 mg/stick, respectively). We also measured 53 additional constituents considered as harmful/carcinogenic. In all cases, the levels were found to be reduced in THS 2.2 aerosol compared to that in 3R4F smoke. The amount of reduction ranged between 64% and 99.9%, with more than 85% reduction in most constituents. These results suggest that THS 2.2 has the potential to reduce HPHC exposure in smokers.

We also measured carbonyl levels in GVP and AE stock solutions generated from mainstream 3R4F and THS 2.2 aerosol. The purpose of these measurements was to monitor the consistency of the smoke/aerosol fractions generated for the different experiments. On the basis of the results from Figure S1, there was little variability among the different fraction generation. Moreover, the results are also in line with those from mainstream smoke/aerosol detailed in Table 2. Most carbonyls showed more than 80% reduction in THS 2.2 aerosol compared to that in 3R4F smoke. Butyraldehyde was the least reduced carbonyl, although the level of reduction compared to 3R4F was still above 50%. Carbonyl values in GVP and AE stock solutions were lower than those in mainstream smoke/aerosol. This was due to differences in the sample preparation protocol. During the initial chemical characterization, mainstream 3R4F smoke and THS 2.2 aerosol were directly trapped and stabilized in DNPH. Since DNPH is highly toxic to NHBE cells, GVP and AE stock solutions were initially prepared in PBS (see Experimental Procedures section), and then, aliquots were stabilized in DNPH. Carbonyls are volatile; therefore, it is likely that some evaporation occurred

between the preparation of the GVP and AE stock solutions and the DNPH stabilization.

Increased Cell Viability in NHBE Cells Exposed to THS 2.2 Aerosol Compared to That in 3R4F Smoke. Cell viability was initially measured using a real-time cellular analysis. This method is based on the use of sensor microelectrodes covering the bottom area of each well in a tissue culture plate.⁵¹ Adherent cells interact with the plate electrodes causing an increase in the electrode's impedance that can be easily measured. The electrode's impedance is dependent on the number of cells attached to the bottom of the well and thus can be used to monitor cell viability. Exposure to all three 3R4F smoke fractions caused a dose- and time-dependent decrease in NHBE cell viability (Figure 1). This effect was already observed at 4 h but was more evident at 24 h. When the 24 h data were fitted by nonlinear regression, the following EC₅₀ values could be calculated for 3R4F: AE (42 puffs/L), TPM (30 puffs/L), and GVP (61 puffs/L). When all three fractions were compared together (Figure S2), TPM showed the highest level of cytotoxicity, followed by AE and finally GVP. In the case of THS 2.2, no major effects were observed upon exposure to even the highest dose of AE (350 puffs/L), TPM (450 puffs/L), or GVP (350 puffs/L). Around 30% decrease in cell viability was observed upon exposure to THS 2.2 AE and TPM for 24 h, but the response was not dose-dependent (Figure 1). These results were further confirmed via HCS. The cell count end point measures the average number of cells that remain attached to the culture plate after exposure. All three 3R4F smoke fractions caused a clear dose-dependent decrease in cell count at 24 h (Figures S3–S5, panel A). By contrast, no changes in cell loss were observed upon exposure to THS 2.2 GVP or TPM

fractions, and only a moderate effect (less than 50% decrease in cell count) was observed at the highest AE concentration after 24 h.

THS 2.2 Aerosol Exhibits Reduced Toxicity in NHBE Cells Compared to That of 3R4F Smoke. The toxic effects of THS 2.2 aerosol and 3R4F smoke were measured using multiple HCS-based assays. A summary of the results for all three smoke/aerosol fractions is listed in Table 3. Exposure to all three 3R4F smoke fractions resulted in a dose-dependent response in most HCS end points. No effects were observed at similar doses of THS 2.2 concentrations; however, a positive response was observed in some cases at higher THS 2.2 concentrations, (Table 3 and Figures S3–S5).

We initially investigated the ability of 3R4F and THS 2.2 to induce DNA damage by measuring the number of cells positively stained for phosphorylated histone 2A variant X (p-H2AX), a well-established marker of DNA double strand breaks.⁵² Exposure to 3R4F TPM caused a dose-dependent increase in p-H2AX at both 4 and 24 h (Figure S4B). A small effect was also observed for THS 2.2 TPM at 24 h but at much higher doses (226 puffs/L) compared to that of 3R4F (8 puffs/L). Exposure for 4 h and 24 h to 3R4F AE and GVP fractions caused an increase in p-H2AX (Figures S3B and S5B), but the effect was only observed at doses that, based on real-time cellular analysis (Figure 1, panel F) and measured cell counts (Figure S3A), induced marked cytotoxicity. No response was observed when NHBE cells were exposed to AE or GVP from THS2.2 (Figures S3B and S5B).

Exposure to all three 3R4F smoke fractions caused a dose-dependent increase in the levels of phosphorylated c-Jun N-terminal kinase at 24 h (Figures S3–S5, panel C), consistent with the presence of cellular or oxidative stress. No effects were observed at comparable doses of the different THS 2.2 aerosol fractions, and only a moderate effect (less than 2-fold increase over the vehicle control) was observed at high concentrations of THS 2.2 AE (200 puffs/L).

Oxidative stress can occur either as a result of increased formation of reactive oxygen species (ROS) or a significant decrease in cellular antioxidant defenses, such as the endogenous antioxidant glutathione (GSH) (Figures S3–S5, panels D–E). Exposure to 3R4F AE at doses above 100 puffs/L caused a moderate increase in ROS formation at 24 h. An effect was also observed for 3R4F GVP, but the response was not dose-dependent and only observed at the highest concentration tested (200 puffs/L). 3R4F TPM could not be evaluated because of the presence of autofluorescence interfering with the assay. All 3R4F smoke fractions caused a dose-dependent decrease in GSH content at both 4 and 24 h. At comparable doses, THS 2.2 fractions did not increase ROS production, although an effect was observed at TPM doses above 350 puffs/L. THS 2.2 AE and GVP fractions also caused a decrease in GSH levels, but only at doses above 200 puffs/L and 350 puffs/L, respectively. Taken together, these results indicate that 3R4F smoke fractions are much stronger inducers of oxidative stress than fractions derived from THS 2.2 aerosol.

The accumulation of DNA or oxidative cellular damage often leads to the activation of cell cycle checkpoints that block cell proliferation until the damage is repaired. We investigated the effects of 3R4F and THS 2.2 on NHBE cell proliferation by cell cycle analysis using a modified thymidine analogue (Figure S6). All smoke/aerosol fractions caused a concentration dependent decrease in the percentage of cells in S-phase and an increase in the percentage of cells in G2-M phase, consistent with the

presence of a cell cycle arrest. However, these effects were observed at lower concentrations of 3R4F smoke (8–25 puffs/L) compared to that of THS 2.2 aerosol (140–200 puffs/L) (Table 3 and Figure S6).

Growth arrest allows cells to repair damage; however, if the cellular insult is severe or prolonged in time, it can permanently damage cellular components (e.g., proteins, lipids, or DNA) and eventually cause cell death. In fact, the results from cell cycle analysis indicated that exposure to 3R4F fractions also caused a dose-dependent increase in the number of apoptotic cells, whereas no apoptosis was observed at comparable THS 2.2 doses (Figure S6). To further investigate the pro-apoptotic effects of 3R4F smoke fractions, we measured two additional markers of apoptosis: the release of cytochrome *c* from the mitochondria and the increase in caspase 3/7 activity (Figures S3–S5, panels F–G).

All three 3R4F smoke fractions caused the release of cytochrome *c* from the mitochondria at 24 h, although in the case of GVP, the effect was observed only at the highest dose tested. Moreover, a moderate increase in caspase 3/7 activity was observed upon exposure to GVP but not to the AE smoke fraction. The effect of 3R4F TPM on caspase activity could not be evaluated owing to the presence of autofluorescence. In the case of THS 2.2, no effects on any of the two end points were observed at comparable doses. A moderate increase in cytochrome *c* release was observed at high concentrations of AE and TPM, and an increase in caspase activity was observed at high concentrations of TPM and GVP.

We evaluated cellular integrity by using YO-PRO-1, a dye that stains the cell only when the cellular membrane becomes permeable, which typically occurs in late apoptotic or necrotic cells. All three 3R4F smoke fractions caused a dose-dependent increase in cell membrane permeability at 4 and 24 h (Figures S3–S5, panel H). No effects were observed for THS 2.2 at comparable doses, although a partial response was observed at high doses (>150 puffs/L) of AE and TPM fractions.

Finally, we investigated the effect of both test items in mitochondrial function using a fluorescent dye (MitoTracker) that allows the measurement of mitochondrial membrane potential and mitochondrial mass (Figures S3–S5, panels I–J). Exposure to TPM caused a decrease in both mitochondrial parameters for both test items, although the effect was observed at lower 3R4F concentrations compared to those of THS 2.2. Exposure to AE from both 3R4F and THS 2.2 caused an increase in mitochondrial potential, but only in the case of 3R4F was this accompanied by a decrease in mitochondrial mass. 3R4F GVP caused an increase in mitochondrial potential at 24 h but only at the highest concentration. In general, only a moderate effect on mitochondrial mass was observed for both items.

Taken together, all of these results indicate that fractions generated from the candidate MRTTP THS 2.2 have a reduced toxicity in NHBE cells compared to fractions generated from the conventional cigarette 3R4F.

Exposure to THS 2.2 Aerosol Fractions Have a Lower Impact on the NHBE Cell Transcriptome Compared to That of 3R4F Smoke Fractions. In order to evaluate the overall effects of THS 2.2 and 3R4F fractions on the transcriptome of NHBE cells, we performed gene expression analysis after 4 h of exposure. We have previously shown that 4 h is an adequate time point to investigate the CS effects on NHBE cell transcriptome.^{36,53} Cells were exposed for 4 h to three different doses of each test item and smoke/aerosol fraction. The highest dose in each case was selected so that at least 60% cell

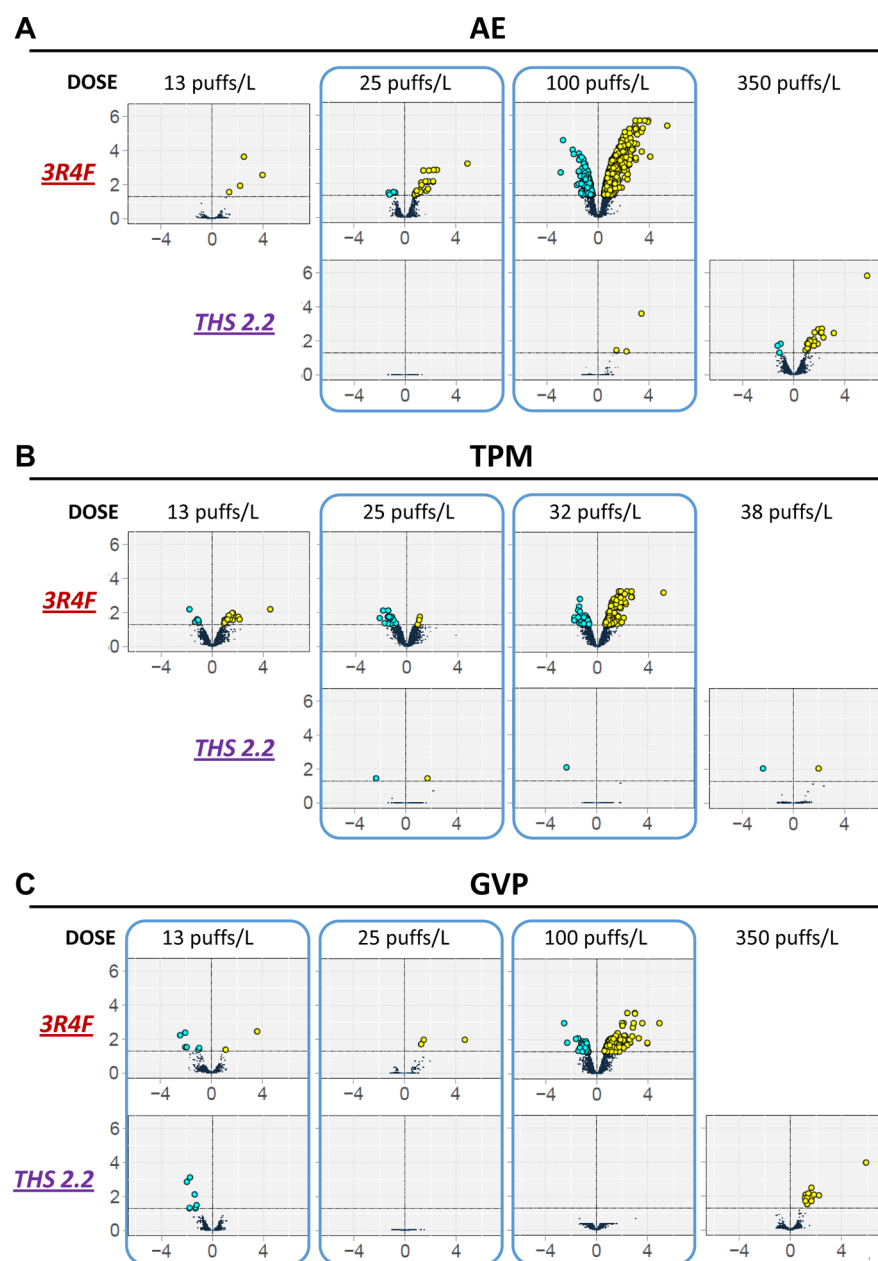


Figure 2. Gene expression changes in NHBE cells exposed for 4 h to AE (A), TPM (B), and GVP (C) fractions generated from 3R4F smoke and THS 2.2 aerosol. For each gene, the gene expression change was calculated as the log₂ FC and the statistical significance as $-\log_{10}(\text{fdr})$. The log₂ FC are shown on the *x* axis. The $-\log_{10}(\text{fdr})$ are shown on the *y* axis. Negative fold-changes are shown in the volcano plots in cyan and positive fold-changes in yellow. Changes below an *fdr* of 0.05 are shown as dark dots.

viability was observed after 24 h of exposure. Additional concentrations were chosen so that the different smoke/aerosol fractions could be compared (Table S2).

For each 3R4F smoke and THS 2.2 aerosol fraction, we determined the changes in gene expression compared to that of the respective controls (Figure 2). For 3R4F, a clear dose-dependent increase in the number of differentially expressed genes was observed in all smoke fractions. A dose-dependent response was also observed for THS 2.2 aerosol in the AE but not in the TPM and GVP fractions. At similar doses of AE (25 puffs/L and 100 puffs/L), TPM (25 puffs/L and 32 puffs/L), and GVP (13 puffs/L, 25 puffs/L, and 100 puffs/L), the number of differentially expressed genes was higher in 3R4F exposed cells compared to that in THS 2.2.

Exposure to THS 2.2 Aerosol Has a Lower Biological Impact in the NHBE Cell Transcriptome Compared to That of 3R4F Smoke. We used ingenuity pathway analysis (IPA) to identify biological pathways that were impacted by the exposure to 3R4F and THS 2.2 (Figure 3). IPA typically requires the use of both FC and *p*-value thresholds. Given the overall low number of differentially expressed genes (DEG) observed in THS 2.2 samples using a *p*-value of 0.05, we decided to increase the *p*-value to 0.1. Even under these conditions, no DEG were found for some THS 2.2 doses (AE, 25 puffs/L; and GVP, 25 puffs/L and 100 puffs/L) and thus, they could not be included in the analysis. For all remaining groups, the most significantly impacted canonical pathway was the NRF2-mediated oxidative stress response. Many other canonical pathways involved in the biosynthesis of endogenous antioxidants, such as glutathione,

Canonical Pathways	AE					GVP					TPM					
	3R4F			THS 2.2		3R4F			THS 2.2		3R4F			THS 2.2		
	13	25	100	100	350	13	25	100	13	350	13	25	32	25	32	38
	puffs/L	puffs/L	puffs/L	puffs/L	puffs/L	puffs/L	puffs/L	puffs/L	puffs/L	puffs/L	puffs/L	puffs/L	puffs/L	puffs/L	puffs/L	puffs/L
NRF2-mediated Oxidative Stress Response	1.77	3.43	0.36		5.83			2.93		2.98	0.45		0.99			
Glutathione Biosynthesis	3.62	2.69	1.22		2.54					3.14	2.16		1.76			
Methylglyoxal Degradation III		2.88		3.32	1.94					2.54	1.56		1.17			
Bile Acid Biosynthesis, Neutral Pathway		1.91	0.55	3.14	1.76					2.36	1.39		1.42			
Unfolded protein response			2.60					3.13					0.47			
Serine Biosynthesis								1.29				2.80				
γ-glutamyl Cycle	2.77	1.85	0.45		1.70					2.30	1.32		0.95			
Superpathway of Serine and Glycine Biosynthesis I								1.16				2.42				
TR/RXR Activation		1.17		2.39	1.27					1.61	0.67	0.23	0.35			
Glutathione Redox Reactions I		1.91			1.76											
Glycolysis I			0.45									1.89				
Endoplasmic Reticulum Stress Pathway			1.86					0.84								
Protein Ubiquitination Pathway			1.81					1.61			0.23		0.76			
LXR/RXR Activation			0.30									0.28	1.80			
Superpathway of Citrulline Metabolism			0.57					1.71					1.80			
Glutamine Degradation I			1.22					1.75					1.76			
G Beta Gamma Signaling		1.73			0.94			0.76			0.58		0.28			
Tetrahydrofolate Salvage from 5,1-methenyltetrahydrofolate			0.57					1.71								
Purine Nucleotides De Novo Biosynthesis II			0.57					1.71								
Polyamine Regulation in Colon Cancer			0.45		1.70			0.93			1.32		0.95			
Inositol Pyrophosphates Biosynthesis			1.69									1.35	1.17			
Gluconeogenesis I			0.37									1.68	0.84			
Role of Tissue Factor in Cancer		1.14	0.48		0.99			0.86			0.64	1.16	1.60			
Interferon Signaling			0.33									1.59	0.80			
Aldosterone Signaling in Epithelial Cells			0.99					1.54					0.52			

Figure 3. Canonical pathways in NHBE cells exposed to 3R4F smoke and THS 2.2 aerosol fractions. IPA analyses were performed using the threshold cutoff $FC > \log_2(1.2)$ and $\text{fdr corrected } p\text{-value} < 0.1$. The results of a comparison analysis between the different groups are shown. Only the top 25 canonical pathways present in at least two groups are included. Darker purple corresponds to stronger statistical significance. The numbers indicate the negative \log_{10} -transformed p -values derived from the Fisher's Exact test. The rows (pathways) with the highest total significances across the groups are sorted at the top.

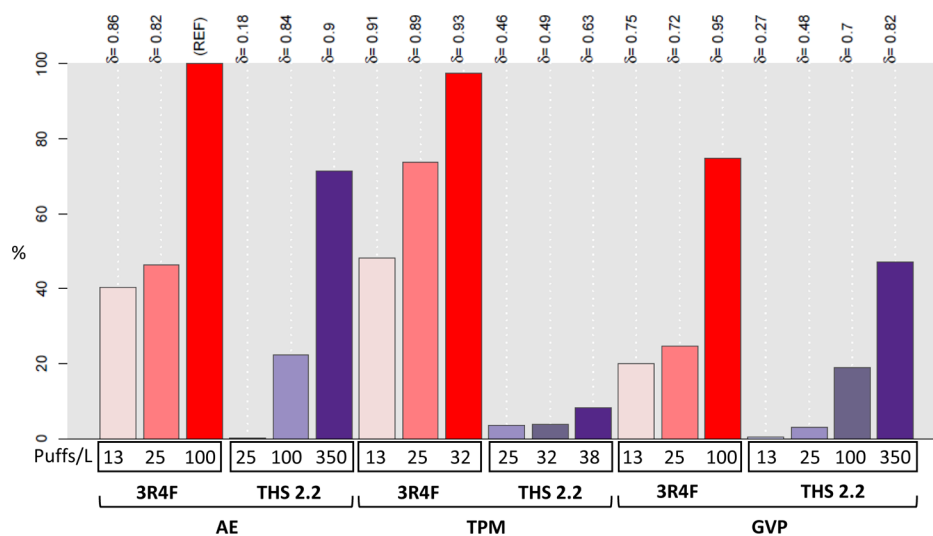


Figure 4. Network model-based analysis of the BIF. The bar plot shows BIF values normalized to both the vehicle control (which is given a 0% value) and the maximum response, which is used as reference (REF) and given a 100% value. The δ values (−1 to 1) indicate how similar the underlying network perturbations are with respect to the REF. Scores were computed using transcriptomics profiling data from 3R4F- and THS 2.2-exposed, NHBE cells compared with vehicle-exposed cells.

were also affected. The number of significantly impacted canonical pathways was higher in 3R4F fractions compared with that in THS 2.2. In fact, all canonical pathways were significantly activated in at least one 3R4F smoke fraction. By contrast, very few canonical pathways were found significantly

activated upon exposure to THS 2.2, except at the highest GVP and AE doses (350 puffs/L).

In order to gain further mechanistic insight into the molecular mechanisms behind the differential toxicity of THS 2.2 and 3R4F, the gene expression data were interpreted through a series

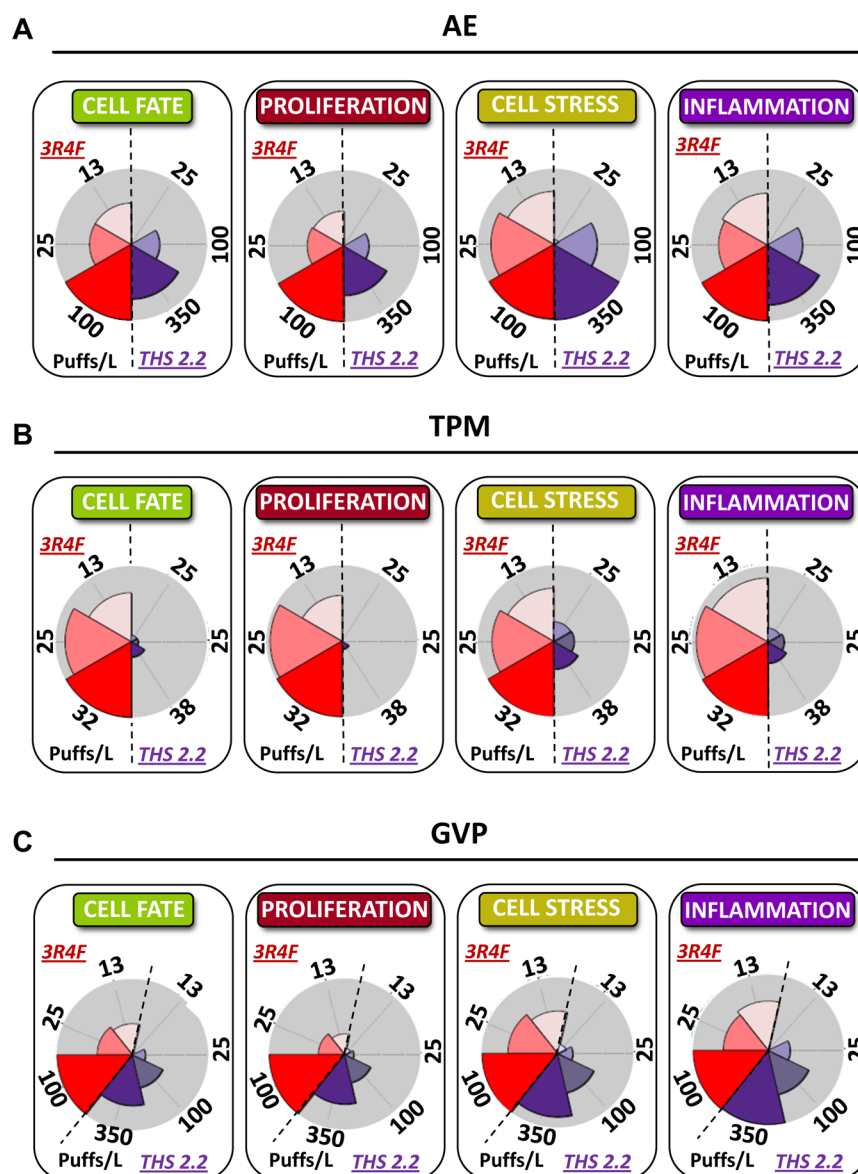


Figure 5. Biological impacts on the network models after 4 h exposure to AE (A), TPM (B), or GVP (C) fractions from 3R4F smoke or THS 2.2 aerosol. The pie chart represents the distribution of the sum of contributions for each network across all treatment groups. The surface area of the different segments within each plot is normalized to the dose showing the maximum level of network perturbation, which is used as a reference. The sum of all contributions for each treatment is 100%. Numbers outside the pie chart indicate the concentration of the different fractions in puffs/L.

of biological networks specifically built for lung and vascular tissue contexts (Table S1). These networks included the following biological processes: cell proliferation,⁴⁴ cellular stress,⁴⁶ inflammatory processes,⁴⁵ and cell fate,⁴⁷ which comprises DNA damage, autophagy, apoptosis, necroptosis, and senescence. Moreover, we used a threshold-free approach, which allowed us to include in the analysis those THS 2.2 AE and GVP doses that could not be used in IPA.

Relative BIF values represent an aggregated biological impact in which a sum of all perturbations across all biological networks is calculated for each treatment. The resulting values are then normalized to both vehicle control, which is assigned a value of 0%, and to the reference, which is defined as the treatment showing the highest level of perturbation and assigned a value of 100%. Figure 4 shows relative BIF values for NHBE cells exposed for 4 h to different concentrations of 3R4F smoke fractions and THS 2.2 aerosol fractions. The reference value used was the 100 puffs/L dose of 3R4F AE, because this was the treatment with the

highest level of overall network perturbation. The values of all other treatments are relative to this reference. The results clearly showed that, for all fractions, the biological impact of 3R4F smoke on NHBE cells is higher than that of THS 2.2 aerosol. At similar doses, the biological impact of any THS 2.2 aerosol fraction was much lower than that in the respective 3R4F smoke fraction. Moreover, the common dose of 25 puffs/L can be used to compare the biological impact of both test items across the different smoke/aerosol fractions (Figure S7). The results suggest that TPM has the highest biological impact among all three 3R4F smoke fractions, followed by AE and finally GVP. In the case of THS 2.2, TPM and GVP showed a higher BIF value than AE. However, these observations should be taken with care, as the overall biological impact of THS 2.2 fractions is very low compared to that of 3R4F.

Relative BIF values can be separated into the different mechanistic components contributing to the overall biological impact, namely, cell fate, proliferation, cell stress, and

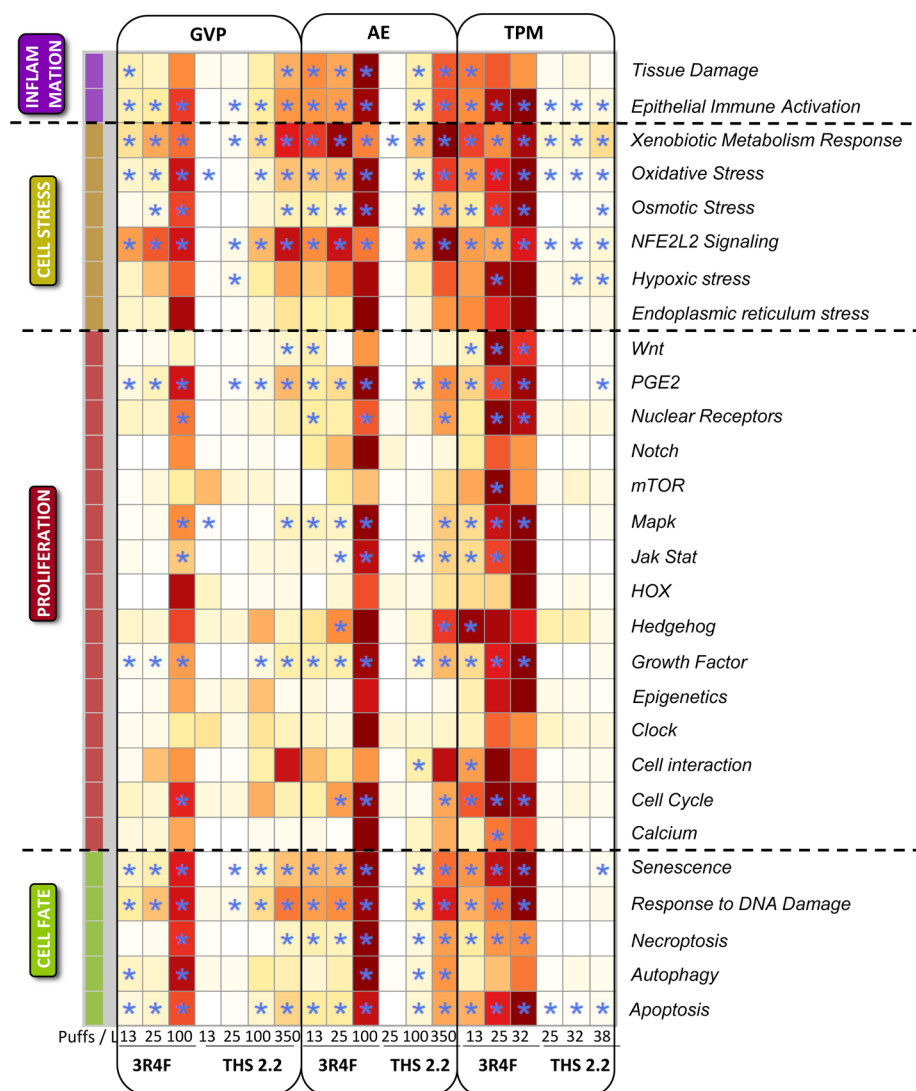


Figure 6. NPA heatmaps for NHBE cells exposed to 3R4F smoke and THS 2.2 aerosol fractions. Darker colors indicate higher NPA scores. Significantly perturbed networks are indicated as *.

inflammation. Figure 5 shows the impact of 3R4F smoke and THS 2.2 aerosol fractions on these four components. Each star plot corresponds to one mechanistic component. The surface area of each segment represents the level of network perturbation caused by the different doses of 3R4F and THS2.2 in that particular component. The areas are normalized to the dose showing the maximum level of network perturbation, which is used as a reference. The results showed that exposure to 3R4F smoke fractions resulted in a higher level of perturbation in all biological networks compared to that of THS 2.2 aerosol fractions.

The mechanistic components contributing to the overall biological impact can be broken down into more specific subnetworks, thus providing more granular mechanistic information. Figure 6 contains a heat map of all the subnetworks that are significantly perturbed in at least one treatment. The level of network perturbation is determined by the NPA score. Values are normalized to the maximum NPA score within each subnetwork and plotted as a color scale. This type of representation allows the comparison of the level of perturbation of a specific subnetwork across different test items, doses, and fractions. In general, exposure to 3R4F resulted in a higher level

of network perturbation and a higher number of perturbed networks than exposure to THS 2.2 aerosol. Most cell fate, cell stress, and inflammation subnetworks were highly perturbed upon exposure to 3R4F smoke, but this was not the case at similar doses of THS 2.2. There were significantly perturbed proliferation subnetworks, but the level of perturbation was also higher in 3R4F compared to that in THS 2.2. At the highest THS 2.2 AE and GVP doses, the perturbation profiles started to resemble those of 3R4F-exposed cells. Interestingly, THS 2.2 TPM fraction caused a very low level of network perturbation at all tested doses. Finally when all fractions are compared using the common dose of 25 puffs/L (Figure S7), the results show that TPM caused the highest level of network perturbation across all 3R4F smoke fractions, followed by AE and GVP. By contrast, all three THS 2.2 aerosol fractions showed a very low level of perturbation.

DISCUSSION

In the present study, we have investigated the toxicity of the candidate MRTTP THS 2.2. Chemical characterization of mainstream THS 2.2 aerosol showed lower levels of HPHCs compared to that of mainstream smoke from the reference

cigarette 3R4F. In addition, exposure to THS 2.2 aerosol fractions resulted in reduced toxicity and an overall lower biological impact on the NHBE cell transcriptome when compared to that of 3R4F smoke fractions.

Contrary to 3R4F, which is a combustible cigarette, the tobacco in THS 2.2 is heated rather than burned. This results in a nicotine containing aerosol that is chemically less complex than CS. Accordingly, the THS 2.2 mainstream aerosol showed a reduction between 64% and 99.9% (85% average reduction) in all measured HPHCs compared to that of 3R4F (Table 2). CS contains liquid droplets (the particulate phase or TPM) suspended in a gas-vapor phase. In terms of composition, both 3R4Fsmoke and THS 2.2 aerosol showed similar TPM values. However, the composition of the particulate phase is also less complex in THS 2.2, with a higher proportion of water and glycerol and a 67% reduction in NFDPM (also known as tar). Interestingly, a different, prototypic MRTTP using a carbon tip to heat tobacco without burning, also showed decreased HPHC levels compared to that of a combustible cigarette.^{53,54} Taken together, these results support the notion that heat-not-burn technologies have the potential to reduce the exposure to many HPHCs in smokers unwilling to quit smoking.

Reduced exposure to toxicants does not necessarily imply reduced toxicity. First, CS contains a large number of constituents⁴ that have not been measured in the study. More importantly, there is no *a priori* knowledge on how much the levels of one or more HPHCs need to be reduced in order to observe a reduction in toxicity. Therefore, in the second part of this article we performed a comprehensive toxicological assessment of THS 2.2 comparing its effects to those of the reference cigarette 3R4F. We followed a systems toxicology approach whereby HCS-based functional toxicity end points were complemented by transcriptomics profiling. Gene expression changes were interpreted using a series of causal biological network models, which allowed us to identify and quantify molecular mechanisms of toxicity that were specifically perturbed by 3R4F smoke or THS 2.2 aerosol fractions. One of the advantages of our approach is that the information can be structured into levels of increasing granularity, thus allowing for a stepwise interpretation of the biological data. The first level of information is the relative BIF, which provides an overview of how much the biological system is impacted by the different experimental conditions. All three 3R4F smoke fractions caused a dose-dependent increase in the overall biological impact (Figure 4). By contrast, exposure to comparable doses of THS 2.2 aerosol resulted in much lower values, with no major differences between the different fractions. These results are in agreement with those from real-time cellular analyses (Figure 1) and HCS-based cell count measurements (Figures S3–S5, panel A) showing a clear cytotoxic effect of 3R4F smoke fractions, whereas little to no effect was observed at even 10-fold higher doses of THS 2.2 aerosol.

The second level of increased granularity results from the separation of the overall impact into its mechanistic components. This type of representation provides quantitative information on the differential effects of 3R4F and THS 2.2 on each of the biological networks. In the case of 3R4F, a clear dose-dependent response was observed in all networks and for all smoke fractions (Figure 5). A dose-dependent response was also observed for THS 2.2 AE and GVP, although the effects in the different networks were always smaller than comparable doses of 3R4F. Little to no effect was observed for THS 2.2. TPM. In fact, even

the lowest dose of 3R4F smoke (13puffs/L) showed a higher impact than the highest dose of THS 2.2 (38 puffs/L).

The third level of granularity results from the decomposition of the biological networks into more specific subnetworks. In this context, NPA scores provide a quantitative measurement of the level of perturbation in each biological network, thus allowing for a more comprehensive interpretation on the underlying molecular mechanisms. CS contains and generates many electrophilic substances that can rapidly react with multiple biological targets.⁵⁵ Exposure to CS also reduces the levels of endogenous antioxidants, including GSH,⁵⁵ leading to the activation of oxidative stress responses.^{56,57} Accordingly, we observed that all 3R4F smoke fractions caused a dose-dependent increase in the level of perturbation in most cell stress subnetworks, including xenobiotic metabolism, oxidative stress, and NFE2L2 (Nrf2) signaling (Figure 6). Similarly, IPA identified NRF2-mediated response and antioxidant biosynthesis as the most significant canonical pathways impacted after exposure to 3R4F fractions. Moreover, 3R4F also caused an increase in ROS formation and a decrease in the levels of the endogenous antioxidant GSH (Table 3 and Figures S3–S5 panel D–E), indicating the presence of oxidative stress. By contrast, exposure to comparable doses of THS 2.2 aerosol fractions resulted in lower perturbation of cell stress subnetworks, lower number of activated IPA canonical pathways, and reduced effects on ROS formation and GSH levels. Increased oxidative stress can cause damage to proteins and DNA.^{55,58,59} Under normal circumstances, the presence of DNA damage causes the activation of cell cycle checkpoints so that cell proliferation is inhibited until the DNA damage is repaired. However, if the damage is left unrepaired, it may ultimately result in the activation of senescence or apoptosis/necrosis programs.^{59–61} Figure 6 shows that most cell fate subnetworks (i.e., senescence, response to DNA repair, and apoptosis) and a number of cell proliferation subnetworks are significantly perturbed in 3R4F exposed cells. By HCS, we observed increased DNA damage in NHBE cells exposed to 3R4F TPM but not to AE and GVP. Nevertheless, cell cycle analysis (Figure S6) showed a decrease in the proportion of cells in S-phase, which indicates that growth arrest is consistent with the presence of oxidative cellular damage. Figure S6 also showed a dose dependent increase in the number of apoptotic cells in response to 3R4F. The presence of apoptosis/necrosis was further supported by the increase in caspase 3/7 activity, cytochrome *c* release, and cellular membrane permeability (Figures S3–S5, panels F, G, and H). However, exposure to THS 2.2 aerosol fractions caused a reduced level of perturbation in cell fate subnetworks compared to that of 3R4F. Furthermore, we found some evidence of growth arrest and apoptosis/necrosis but only at doses one order of magnitude higher than those of 3R4F. Taken together, these findings indicate that in this experimental setup, THS 2.2 aerosol is less toxic to NHBE cells than 3R4F smoke. These results are in line with a previous study that also showed reduced toxicity in NHBE cells exposed to another prototypic MRTTP compared to conventional products,⁵³ suggesting that heat-not-burn technologies may also have the potential to reduce CS-associated risks. Nevertheless, additional and complementary studies are necessary to further test this hypothesis. On the one hand, the use of NHBE cells from additional donors would be helpful to confirm our findings and to investigate inter individual variability. On the other hand, the use of additional relevant *in vitro* models, such as the cardiovascular system or the liver, could also provide

valuable information regarding the biological impact of MRTPs on other target tissues.

■ CONCLUSIONS

The results show that our systems toxicology approach provides robust mechanistic insight into the biological effects of THS 2.2 and 3R4F, and thus, it is useful for the toxicological assessment of candidate MRTPs. Moreover, this type of approach is in line with the “21st century toxicology” paradigm,⁶² which aims for a mechanism-driven toxicological assessment. *In vitro* models represent human biology only to a certain extent and have limitations in terms of exposure duration. Nevertheless, the possibility to simultaneously testing multiple experimental conditions is seen as an important advantage over *in vivo* studies.

Future studies should evaluate the toxicity of THS 2.2 over longer periods of time and upon repeated (chronic or subchronic) exposures. In this context, the use of three-dimensional lung organotypic cultures represents an advantage. Though technically more challenging, these tissue cultures can remain viable and functional for long periods of time, and the presence of an air–liquid interface allows the exposure of cells to mainstream CS, which better resembles human smoking behavior.²¹

■ ASSOCIATED CONTENT

■ Supporting Information

Supporting Information available: This material is available free of charge via the Internet at <http://pubs.acs.org/>. The Supporting Information is available free of charge on the ACS Publications website at DOI: 10.1021/acs.chemrestox.5b00321.

Carbonyl measurements in GVP and AE fractions, cell viability across smoke/aerosol fractions, HCS results in NHBE cells exposed to AE, TPM, and GVP from 3R4F smoke and THS 2.2 aerosol, NPA heatmaps for NHBE cells exposed to AE, TPM, and GVP from 3R4F smoke and THS 2.2 aerosol, biological networks and subnetworks used in the study, and selected doses for to generate gene expression data (PDF)

■ AUTHOR INFORMATION

Corresponding Author

*E-mail: Ignacio.GonzalezSuarez@pmi.com.

Funding

The research described in this article was funded by Philip Morris International.

Notes

The authors declare the following competing financial interest(s): All authors are employees of Philip Morris International. Philip Morris International is the sole source of funding and sponsor of this project.

■ ACKNOWLEDGMENTS

We thank Filippo Zanetti and Maurice Smith for a critical review of the manuscript, Vincenzo Belcastro for the submission of the gene expression data to ArrayExpress, and Daniella Keller for providing a description of the chemical characterization methods.

■ ABBREVIATIONS

AE, aqueous extract; BIF, biological impact factor; GSH, glutathione; GVP, gas-vapor phase; HCS, high content screen-

ing; HPHC, harmful or potentially harmful constituent; LOQ, limit of quantification; MRTP, modified-risk tobacco product; NAB, *N'*-nitrosoanabasine; NAT, *N'*-nitrosoanatabine; NFDPM, nicotine-free dry particulate matter; NHBE, normal human bronchial epithelial cells; NNK, *N*-nitrosamines, including 4-(methylnitrosamino)-1-(3-pyridyl)-1-butanone; NNN, *N'*-nitrosonornicotine; NO, NO_x, nitric oxide, nitric oxides; NPA, network perturbation amplitude; PBS, phosphate buffered saline; pH2AX, phosphorylated histone H2AX; ROS, reactive oxygen species; THS, tobacco heating system; TPM, total particulate matter

■ REFERENCES

- (1) (2014) *The Health Consequences of Smoking: 50 Years of Progress: A Report of the Surgeon General*, U.S. Department of Health and Human Services, National Center for Chronic Disease Prevention and Health Promotion, Office on Smoking and Health, Atlanta, GA.
- (2) (2012) *Modified Risk Tobacco Product Applications: Draft Guidance for Industry*, Food and Drug Administration, Silver Springs, MD.
- (3) Baker, R. R. (1974) Temperature distribution inside a burning cigarette. *Nature* 247, 405–406.
- (4) Rodgman, A., and Perfetti, T. A. (2013) *The Chemical Components of Tobacco and Tobacco Smoke*. 2nd ed., CRC Press, Taylor & Francis Group, Boca Raton, FL.
- (5) (2012) *Harmful and Potentially Harmful Constituents in Tobacco Products and Tobacco Smoke; Established List*, pp 20034–20037, US Food and Drug Administration, Silver Springs, MD.
- (6) (2010) *How Tobacco Smoke Causes Disease: The Biology and Behavioral Basis for Smoking-Attributable Disease: A Report of the Surgeon General*, Office on Smoking and Health, U.S. Department of Health and Human Services, Atlanta, GA.
- (7) (2007) *Smokeless Tobacco and Some Tobacco-Specific N-Nitrosamines*, International Agency for Research on Cancer (IARC), Lyon, France.
- (8) Beane, J., Sebastiani, P., Liu, G., Brody, J. S., Lenburg, M. E., and Spira, A. (2007) Reversible and permanent effects of tobacco smoke exposure on airway epithelial gene expression. *Genome Biol.* 8, R201.
- (9) Burns, D. M., Dybing, E., Gray, N., Hecht, S., Anderson, C., Sanner, T., O'Connor, R., Djordjevic, M., Dresler, C., Hainaut, P., Jarvis, M., Oppenhuizen, A., and Straif, K. (2008) Mandated lowering of toxicants in cigarette smoke: a description of the World Health Organization TobReg proposal. *Tob. Control* 17, 132–141.
- (10) Ding, Y. S., Ashley, D. L., and Watson, C. H. (2007) Determination of 10 carcinogenic polycyclic aromatic hydrocarbons in mainstream cigarette smoke. *J. Agric. Food Chem.* 55, 5966–5973.
- (11) Ding, Y. S., Yan, X. J., Jain, R. B., Lopp, E., Tavakoli, A., Polzin, G. M., Stanfill, S. B., Ashley, D. L., and Watson, C. H. (2006) Determination of 14 polycyclic aromatic hydrocarbons in mainstream smoke from U.S. brand and non-U.S. brand cigarettes. *Environ. Sci. Technol.* 40, 1133–1138.
- (12) Fujioka, K., and Shibamoto, T. (2006) Determination of toxic carbonyl compounds in cigarette smoke. *Environ. Toxicol.* 21, 47–54.
- (13) Gregg, E., Hill, C., Hollywood, M., Kearney, M., MacAdam, K., MacLaughlin, D., Purkis, S., and Williams, M. (2004) The UK Smoke Constituents Testing Study. Summary of Results and Comparison with Other Studies. *Beitr. Tabakforsch. Int.* 21, 117–138.
- (14) Mohapatra, P., Preet, R., Das, D., Satapathy, S. R., Siddharth, S., Choudhuri, T., Wyatt, M. D., and Kundu, C. N. (2014) The contribution of heavy metals in cigarette smoke condensate to malignant transformation of breast epithelial cells and *in vivo* initiation of neoplasia through induction of a PI3K-AKT-NFκB cascade. *Toxicol. Appl. Pharmacol.* 274, 168–179.
- (15) Pappas, R. S., Fresquez, M. R., Martone, N., and Watson, C. H. (2014) Toxic metal concentrations in mainstream smoke from cigarettes available in the USA. *J. Anal. Toxicol.* 38, 204–211.
- (16) Poirier, M., Fournier, M., Brousseau, P., and Morin, A. (2002) Effects of volatile aromatics, aldehydes, and phenols in tobacco smoke

on viability and proliferation of mouse lymphocytes. *J. Toxicol. Environ. Health, Part A* 65, 1437–1451.

(17) Werley, M. S., Freelin, S. A., Wrenn, S. E., Gerstenberg, B., Roemer, E., Schramke, H., Van Miert, E., Vanscheeuwijck, P., Weber, S., and Coggins, C. R. (2008) Smoke chemistry, in vitro and in vivo toxicology evaluations of the Electrically Heated Cigarette Smoking System Series K. *Regul. Toxicol. Pharmacol.* 52, 122–139.

(18) Schorp, M. K., Tricker, A. R., and Dempsey, R. (2012) Reduced exposure evaluation of an Electrically Heated Cigarette Smoking System. Part 1: Non-clinical and clinical insights. *Regul. Toxicol. Pharmacol.* 64 (Suppl. 1), S1–S10.

(19) Coggins, C. R., Ayres, P. H., Mosberg, A. T., Sagartz, J. W., Burger, G. T., and Hayes, A. W. (1989) Ninety-day inhalation study in rats, comparing smoke from cigarettes that heat tobacco with those that burn tobacco. *Toxicol. Sci.* 13, 460–483.

(20) Food and Drug Administration, F. (2012) Harmful and potentially harmful constituents in tobacco products and tobacco smoke; established list. *Fed. Regist.* 77, 20034–20037.

(21) Mathis, C., Poussin, C., Weisensee, D., Gebel, S., Hengstermann, A., Sewer, A., Belcastro, V., Xiang, Y., Ansari, S., Wagner, S., Hoeng, J., and Peitsch, M. C. (2013) Human bronchial epithelial cells exposed in vitro to cigarette smoke at the air-liquid interface resemble bronchial epithelium from human smokers. *Am. J. Physiol. Lung Cell Mol. Physiol.* 304, L489–503.

(22) Jorgensen, E. D., Dozmorov, I., Frank, M. B., Centola, M., and Albino, A. P. (2004) Global gene expression analysis of human bronchial epithelial cells treated with tobacco condensates. *Cell Cycle* 3, 1152–1166.

(23) Nyunoya, T., Mebratu, Y., Contreras, A., Delgado, M., Chand, H. S., and Tesfaigzi, Y. (2014) Molecular processes that drive cigarette smoke-induced epithelial cell fate of the lung. *Am. J. Respir. Cell Mol. Biol.* 50, 471–482.

(24) Pickett, G., Seagrave, J., Boggs, S., Polzin, G., Richter, P., and Tesfaigzi, Y. (2010) Effects of 10 cigarette smoke condensates on primary human airway epithelial cells by comparative gene and cytokine expression studies. *Toxicol. Sci.* 114, 79–89.

(25) Sen, B., Mahadevan, B., and DeMarini, D. M. (2007) Transcriptional responses to complex mixtures: a review. *Mutat. Res. Rev. Mutat. Res.* 636, 144–177.

(26) Yauk, C. L., Williams, A., Buick, J. K., Chen, G., Maertens, R. M., Halappanavar, S., and White, P. A. (2012) Genetic toxicology and toxicogenomic analysis of three cigarette smoke condensates in vitro reveals few differences among full-flavor, blonde, and light products. *Environ. Mol. Mutagen.* 53, 281–296.

(27) Hoeng, J., Deehan, R., Pratt, D., Martin, F., Sewer, A., Thomson, T. M., Drubin, D. A., Waters, C. A., de Graaf, D., and Peitsch, M. C. (2012) A network-based approach to quantifying the impact of biologically active substances. *Drug Discovery Today* 17, 413–418.

(28) Hoeng, J., Talikka, M., Martin, F., Sewer, A., Yang, A., Iskandar, A., Schlage, W. K., and Peitsch, M. C. (2014) Case study: The role of mechanistic network models in systems toxicology. *Drug Discovery Today* 19, 183–192.

(29) Thomson, T. M., Sewer, A., Martin, F., Belcastro, V., Frushour, B., Gebel, S., Park, J., Schlage, W. K., Talikka, M., Vasilyev, D., Westra, J. W., Hoeng, J., and Peitsch, M. C. (2013) Quantitative assessment of biological impact using transcriptomic data and mechanistic network models. *Toxicol. Appl. Pharmacol.* 272, 863–878.

(30) (2011) ISO Standard 4387:2000. Cigarettes: Determination of Total and Nicotine Free Dry Particulate Matter Using a Routine Analytical Smoking Machine, International Organization for Standardization (ISO), Genève, Switzerland.

(31) (2010) ISO 8454:2007, Cigarettes: Determination of Carbon Monoxide in the Vapour Phase of Cigarette Smoke: NDIR method, International Organization for Standardization (ISO), Genève, Switzerland.

(32) (2013) ISO 10315:2013, Cigarettes: Determination of Nicotine in Smoke Condensates: Gas-Chromatographic Method, International Organization for Standardization (ISO), Genève, Switzerland.

(33) (1999) ISO 14644–1:1999, Cleanrooms and Associated Controlled Environments, International Organization for Standardization (ISO), Genève, Switzerland.

(34) Lechner, J. F., McClendon, I. A., LaVeck, M. A., Shamsuddin, A. M., and Harris, C. C. (1983) Differential control by platelet factors of squamous differentiation in normal and malignant human bronchial epithelial cells. *Cancer Res.* 43, 5915–5921.

(35) Marescotti, D., Gonzalez Suarez, I., Acali, S., John, S., Laurent, A., Frentzel, S., Hoeng, J., and Peitsch, M. (2015) High Content Screening Analysis To Evaluate The Toxicological Effects Of Harmful And Potentially Harmful Constituents (HPHC). *J. Vis. Exp.*

(36) Gonzalez-Suarez, I., Sewer, A., Walker, P., Mathis, C., Ellis, S., Woodhouse, H., Guedj, E., Dulize, R., Marescotti, D., Acali, S., Martin, F., Ivanov, N. V., Hoeng, J., and Peitsch, M. C. (2014) Systems biology approach for evaluating the biological impact of environmental toxicants in vitro. *Chem. Res. Toxicol.* 27, 367–376.

(37) McCall, M. N., Bolstad, B. M., and Irizarry, R. A. (2010) Frozen robust multiarray analysis (fRMA). *Biostatistics* 11, 242–253.

(38) Dai, M., Wang, P., Boyd, A. D., Kostov, G., Athey, B., Jones, E. G., Bunney, W. E., Myers, R. M., Speed, T. P., Akil, H., Watson, S. J., and Meng, F. (2005) Evolving gene/transcript definitions significantly alter the interpretation of GeneChip data. *Nucleic Acids Res.* 33, e175.

(39) Bolstad, B. M., Irizarry, R. A., Astrand, M., and Speed, T. P. (2003) A comparison of normalization methods for high density oligonucleotide array data based on variance and bias. *Bioinformatics* 19, 185–193.

(40) Gautier, L., Cope, L., Bolstad, B. M., and Irizarry, R. A. (2004) affy-analysis of Affymetrix GeneChip data at the probe level. *Bioinformatics* 20, 307–315.

(41) Smyth, G. K. (2004) Linear models and empirical bayes methods for assessing differential expression in microarray experiments. *Stat. Appl. Genet. Mol. Biol.* 3, 110.2202/1544-6115.1027

(42) Warnes, G. R., Bolker, B. M., Bonebakker, L., Gentleman, R., Huber, W., and Liaw, A. (2012) Various R Programming Tools for Plotting Data. <http://CRAN.R-project.org/package=gplots>

(43) Team, R. D. C. (2012) R: A Language and Environment for Statistical Computing, R Foundation for Statistical Computing, Vienna, Austria.

(44) Westra, J. W., Schlage, W. K., Frushour, B. P., Gebel, S., Catlett, N. L., Han, W., Eddy, S. F., Hengstermann, A., Matthews, A. L., Mathis, C., Lichtner, R. B., Poussin, C., Talikka, M., Veljkovic, E., Van Hooser, A. A., Wong, B., Maria, M. J., Peitsch, M. C., Deehan, R., and Hoeng, J. (2011) Construction of a computable cell proliferation network focused on non-diseased lung cells. *BMC Syst. Biol.* 5, 105.

(45) Westra, J. W., Schlage, W. K., Hengstermann, A., Gebel, S., Mathis, C., Thomson, T., Wong, B., Hoang, V., Veljkovic, E., Peck, M., Lichtner, R. B., Weisensee, D., Talikka, M., Deehan, R., Hoeng, J., and Peitsch, M. C. (2013) A modular cell-type focused inflammatory process network model for non-diseased pulmonary tissue. *Bioinf. Biol. Insights* 7, 167–192.

(46) Schlage, W. K., Westra, J. W., Gebel, S., Catlett, N. L., Mathis, C., Frushour, B. P., Hengstermann, A., Van Hooser, A., Poussin, C., Wong, B., Lietz, M., Park, J., Drubin, D., Veljkovic, E., Peitsch, M. C., Hoeng, J., and Deehan, R. (2011) A computable cellular stress network model for non-diseased pulmonary and cardiovascular tissue. *BMC Syst. Biol.* 5, 168.

(47) Gebel, S., Lichtner, R. B., Frushour, B., Schlage, W. K., Hoang, V., Talikka, M., Hengstermann, A., Mathis, C., Veljkovic, E., Peck, M., Peitsch, M. C., Deehan, R., Hoeng, J., and Westra, J. W. (2013) Construction of a computable network model for DNA damage, autophagy, cell death, and senescence. *Bioinf. Biol. Insights* 7, 97–117.

(48) Boue, S., Talikka, M., Westra, J. W., Hayes, W., Di Fabio, A., Park, J., Schlage, W. K., Sewer, A., Fields, B., Ansari, S., Martin, F., Veljkovic, E., Kenney, R., Peitsch, M. C., and Hoeng, J. (2015) Causal biological network database: a comprehensive platform of causal biological network models focused on the pulmonary and vascular systems. *Database* 2015, bav030.

(49) Martin, F., Sewer, A., Talikka, M., Xiang, Y., Hoeng, J., and Peitsch, M. C. (2014) Quantification of biological network

perturbations for mechanistic insight and diagnostics using two-layer causal models. *BMC Bioinf.* 15, 238.

(50) Martin, F., Thomson, T. M., Sewer, A., Drubin, D. A., Mathis, C., Weisensee, D., Pratt, D., Hoeng, J., and Peitsch, M. C. (2012) Assessment of network perturbation amplitudes by applying high-throughput data to causal biological networks. *BMC Syst. Biol.* 6, 54.

(51) ACEABiosciences (2013) Application Note 1. Real-Time and Dynamic Monitoring of Cell Proliferation and Viability for Adherent Cells, ACEA Biosciences Inc., San Diego, CA.

(52) Lowndes, N. F., and Toh, G. W. (2005) DNA repair: the importance of phosphorylating histone H2AX. *Curr. Biol.* 15, R99–R102.

(53) Kogel, U., Gonzalez Suarez, I., Xiang, Y., Dossin, E., Guy, P. A., Mathis, C., Marescotti, D., Goedertier, D., Martin, F., Peitsch, M. C., and Hoeng, J. (2015) Biological Impact of Cigarette Smoke compared to an Aerosol produced from a Prototypic Modified Risk Tobacco Product on Normal Human Bronchial Epithelial Cells. *Toxicol. In Vitro* 29, 2102–2115.

(54) Patskan, G., and Reininghaus, W. (2003) Toxicological evaluation of an electrically heated cigarette. Part 1: Overview of technical concepts and summary of findings. *J. Appl. Toxicol.* 23, 323–328.

(55) Aoshiba, K., and Nagai, A. (2003) Oxidative stress, cell death, and other damage to alveolar epithelial cells induced by cigarette smoke. *Tob. Induced Dis.* 1, 219–226.

(56) Pierrou, S., Broberg, P., O'Donnell, R. A., Pawlowski, K., Virtala, R., Lindqvist, E., Richter, A., Wilson, S. J., Angco, G., Möller, S., Bergstrand, H., Koopmann, W., Wieslander, E., Stromstedt, P. E., Holgate, S. T., Davies, D. E., Lund, J., and Djukanovic, R. (2007) Expression of genes involved in oxidative stress responses in airway epithelial cells of smokers with chronic obstructive pulmonary disease. *Am. J. Respir. Crit. Care Med.* 175, 577–586.

(57) Muller, T., and Hengstermann, A. (2012) Nrf2: friend and foe in preventing cigarette smoking-dependent lung disease. *Chem. Res. Toxicol.* 25, 1805–1824.

(58) Chen, Z., Wang, D., Liu, X., Pei, W., Li, J., Cao, Y., Zhang, J., An, Y., Nie, J., and Tong, J. (2015) Oxidative DNA damage is involved in cigarette smoke-induced lung injury in rats. *Environ. Health Prev. Med.* 20, 318–324.

(59) Zhao, H., Albino, A. P., Jorgensen, E., Traganos, F., and Darzynkiewicz, Z. (2009) DNA damage response induced by tobacco smoke in normal human bronchial epithelial and A549 pulmonary adenocarcinoma cells assessed by laser scanning cytometry. *Cytometry, Part A* 75, 840–847.

(60) van der Toorn, M., Rezayat, D., Kauffman, H. F., Bakker, S. J., Gans, R. O., Koeter, G. H., Choi, A. M., van Oosterhout, A. J., and Slebos, D. J. (2009) Lipid-soluble components in cigarette smoke induce mitochondrial production of reactive oxygen species in lung epithelial cells. *Am. J. Physiol. Lung Cell Mol. Physiol.* 297, L109–114.

(61) Ahmad, T., Sundar, I. K., Lerner, C. A., Gerloff, J., Tormos, A. M., Yao, H., and Rahman, I. (2015) Impaired mitophagy leads to cigarette smoke stress-induced cellular senescence: implications for chronic obstructive pulmonary disease. *FASEB J.* 29, 2912–2929.

(62) (2007) *Toxicity Testing in the 21st Century: A Vision and a Strategy*, The National Academies Press, Washington, DC.